

In search for the Local Universe dynamical homogeneity scale with CF4++ peculiar velocities

H.M. Courtois^{*1}, J. Mould^{2,3}, A.M. Hollinger¹, A. Dupuy⁴, C.P. Zhang⁵

¹ Université Claude Bernard Lyon 1, IUF, IP2I Lyon, 4 rue Enrico Fermi, 69622 Villeurbanne, France

² Centre for Astrophysics & Supercomputing, Swinburne University, Hawthorn, VIC 3122, Australia

³ ARC Centre of Excellence for Dark Matter Particle Physics

⁴ Korea Institute for Advanced Study, 85, Hoegi-ro, Dongdaemun-gu, Seoul 02455, Republic of Korea

⁵ National Astronomical Observatories, Chinese Academy of Sciences, Beijing 100101, China

Received A&A 2024; Accepted date

ABSTRACT

This article explores a groundbreaking update to the cosmography of the local Universe within $z = 0.1$, incorporating galaxy peculiar velocity datasets from the first data releases of WALLABY, FAST and DESI surveys. The galaxies with peculiar velocities currently selected in each survey is 655, 4796 and 4191 respectively. The new CF4++ compendium enables a more comprehensive study of the nearby Universe bulk flow dynamics. This analysis reveals that the dynamical scale of homogeneity is not yet reached in the interval [200-300] h^{-1} Mpc from the observer. This new data also refines the structure of local superclusters, revealing more spherical shapes and more clearly defined boundaries for key regions such as Great Attractor (Laniakea) and Coma. Very few measurements make a big difference in revealing the hidden Vela supercluster.

Key words. Cosmology: large-scale structure of Universe

1. Introduction

Near-field cosmology explores the structure, dynamics, and evolution of the Universe on relatively small scales within the redshifts $z < 0.1$. A crucial tool in this domain is the analysis of peculiar velocity datasets, which capture the deviations of galaxies' motions from the Hubble flow due to gravitational interactions. By studying these peculiar velocities, we can infer the distribution of mass, both visible and dark, within the local cosmic volume. This allows for detailed examinations of the density field, the local matter power spectrum, and tests of cosmological models and alternative theories of gravity. Peculiar velocity measurements also complement large-scale observations, such as cosmic microwave background and redshift surveys, by constraining parameters like the growth rate of structure formation and the amplitude of matter clustering σ_8 .

The bulk flow as a cosmological probe refers to the coherent motion of galaxies within a specific volume of the universe, driven by gravitational interactions with the large-scale distribution of matter. In the local Universe, this motion represents a deviation from the expected uniform expansion of the Hubble flow, providing a unique diagnostic of the matter distribution, including dark matter, on scales of tens to hundreds of megaparsecs.

The study of the bulk flow in the local Universe provides insights into the scale of gravitational influences, the validity of the standard Λ CDM cosmological model, and potential deviations such as anisotropies or departures from Gaussianity in the primordial density field.

Measurements of the bulk flow are typically derived from peculiar velocity datasets, which quantify the velocity of galaxies relative to the smooth expansion of the universe. These velocities

are obtained through various observational techniques, including distance-independent indicators like the Tully-Fisher relation or the fundamental plane (Nusser & Davis 2011; Hong et al. 2014; Scrimgeour et al. 2016; Qin 2021; Qin et al. 2021; Avila et al. 2023) and supernovae Ia luminosities (Colin et al. 2011; Dai et al. 2011; Turnbull et al. 2012; Boruah et al. 2020; Lopes et al. 2024), combination of several distance indicators in composite catalogs (Watkins et al. 2009; Hoffman et al. 2015; Qin et al. 2019; Boruah et al. 2020; Courtois et al. 2023a; Watkins et al. 2023; Whitford et al. 2023; Boubel et al. 2024) or redshift surveys (Carrick et al. 2015; Stahl et al. 2021).

This article presents an updated cosmography of the local Universe within $z = 0.1$ using the composite catalog CosmicFlows-4 upgraded by the addition of 9,642 galaxies from the first data releases of WALLABY, FAST and DESI surveys, called CF4++. We first present the building of the CF4++ dataset in section 2, and the updated local Universe density and gravitational velocity fields reconstruction in section 3. Section 4 delivers the analysis of the bulk flow in the Local Universe and conclusions are drawn in section 5.

2. Integration of recent peculiar velocity datasets

2.1. WALLABY Pilot Survey

The Widefield ASKAP L-band Legacy All-sky Blind survey (WALLABY; Koribalski et al. 2020) SKA pilot survey recently released its first set of public data, marking a significant milestone for the project (Westmeier et al. (2022), Murugesan et al. (2024)). Conducted using the Australian Square Kilometre Array Pathfinder (ASKAP), WALLABY aims to map neutral hydrogen (HI) across the southern hemisphere. This data release includes HI spectral line cubes and catalogs from three pilot sur-

* h.courtois@ip2i.in2p3.fr

vey regions, providing detailed information on galaxy distributions, dynamics, and gas content.

These observations offer valuable insights into galaxy evolution, large-scale structure, and cosmic flows. The release also serves as a testbed for data processing and analysis pipelines in preparation for larger SKA-scale surveys. Researchers worldwide can now explore this publicly available dataset to conduct their own studies and collaborate on advancing our understanding of the Universe. In Courtois et al. (2023b) and Mould et al. (2024), we have shown how to transform the WALLABY pilot survey data into distance moduli that can be later interpreted as peculiar velocities. In this article we use 655 WALLABY galaxy peculiar velocities.

2.2. FAST DR1 Dataset

The 2024 data release from the Five-hundred-meter Aperture Spherical Telescope (FAST; Zhang et al. 2024) represents a significant milestone in radio astronomy. This release, part of the FAST All-Sky HI Survey (FASHI), includes a catalog of over 41,700 extragalactic neutral hydrogen (HI) sources, making it one of the largest HI survey on a single telescope dataset. With a sensitivity and resolution superior to previous surveys, such as ALFALFA, the data enable detailed studies of galaxy dynamics, star formation, and the large-scale structure of the Universe. The survey also provides crucial cross-matched catalogs linking FAST data to optical sources, further enhancing its scientific utility.

This publicly available dataset not only supports cosmological research but also sets the stage for groundbreaking studies in galaxy formation and evolution, as well as follow-ups using FAST's advanced capabilities. By releasing this unprecedented dataset, FAST solidifies its role as a leading facility in global radio astronomy

Zhang et al. (2024) have provided optical identification for 10,976 of their sources with the Siena Galaxy Atlas (SGA; Moustakas et al. 2023). From the grz photometry of the SGA we chose the z band for the Tully Fisher Relation (TFR), because of its lesser problems with internal galactic extinction. The SGA authors used profile fitting to obtain total magnitudes for their galaxies, simultaneously solving for ellipticity, and they catalog axial ratios, which are necessary for the TFR. Zhang et al. (2024) have compared their detection velocities with those of the ALFALFA survey (Haynes et al. 2018), finding good agreement. We compared their $w50$ values with those of ALFALFA and also found good agreement using 1938 galaxies.

For measuring distances, CF4 uses the baryonic TFR. In order to incorporate the FAST galaxies we used the $g-r$ colour to derive the galaxy's M_*/L_z from equation (1) of Taylor et al. (2015) modified using,

$$g-i = 1.408(g-r-0.753)+1.14 \quad \text{and} \quad i-z = 0.03(g-r-0.753)+0.235$$

obtained from tight colour-colour relations fitted to $ugriz$ photometry of Hydra galaxies by Lima-Dias et al. (2021). The adopted relation is,

$$\log M_* = 0.974(g-r) + 0.802 - 0.4M_z.$$

We normalized the M_* values so obtained to those of 850 galaxies in the FAST-SGA sample that also appear in the CF4 catalogue. This normalization has an uncertainty of 0.0046 dex. We similarly normalized the FAST HI masses to the gas masses of the CF4 catalogue with an uncertainty of 0.018 dex. The combined uncertainty of the zeropoint of the baryonic TFR closer to

the M_* zeropoint uncertainty than the gas mass uncertainty as galaxies on average have a gas mass less than their stellar mass. This normalization also brings the data into conformity with the Hubble Constant present in the CF4 catalogue.

Galaxies with 2.5σ disagreements between FAST/Siena and CF4 are rejected from the sample. Objects with fractional FAST $w50$ errors exceeding 4.7% were also rejected. The z band magnitudes were corrected for extinction using the Caltech-IPAC E(B-V) values for each galaxy individually (Schlafly & Finkbeiner 2011). These are small corrections. The biggest E(B-V) was 0.2 and the median < 0.02 mag. $A_z/E(B-V) = 1.263$. Finally, some galaxies were removed from the distance measurement sample as 2.5σ deviants from the TFR fit.

2.2.1. Analysis of galaxies identified with Sloan Digital Sky Survey galaxies

Some 14,070 FAST galaxies are identified with SDSS objects. We cross-matched these objects with DELVE DR2 objects from the DECam Local Volume Exploration Survey (DELVE DR2 catalog; Drlica-Wagner et al. 2022) with a matching radius of $7''$. Based on images with the Dark Energy Camera at Cerro Tololo in Chile, DELVE has limited coverage of the northern hemisphere. Galaxies with 2.5σ deviations from the fitted relation $y = 10.39 + 3(x - 2.405)$ were discarded from the distance sample.

The baryonic TFR normalization of M_* was done using the full sample of DELVE DR2 galaxies that are in the CF4 catalogue, only one of which is a FAST detection. This zeropoint is determined by 54 galaxies to 0.06 dex in $\log M_*$, but nevertheless secures a value of H_0 for the 350 galaxies SDSS sample, which is the same as for the CF4 catalogue. This assures us that spurious large scale flow fields are not added to the CF4 dataset.

2.2.2. Identifications from DELVE DR2 alone

In the previous sections we have used the positional information from identifications made by (Zhang et al. 2024) to cross match with optically catalogued galaxies. We now attempt to match some of the non-SGA and non-SDSS FAST 2023 sources with DELVE DR2 galaxies. We tested acceptance radii of 0.18 arcmin, 0.24 arcmin and 0.27 arcmin. In this mass-radius relation there is a tendency for spurious objects to fall below the lower envelope of the real ones. None of the chosen radii seem to fail this condition, however.

The Legacy Survey¹ as part of DR9 has provided Tractor photometry of northern fields, and we have matched these with FAST sources in the same way as for the DELVE survey. We included every object with $z < 22$ and half light radius greater than $3''$. The mass radius relations looks the same as for the DELVE identifications, with the same independence on matching radius out to 2.7 arcmin. We chose the zeropoint of the Tractor photometry to match that of the SGA photometry. With over 2000 galaxies this was achieved to an accuracy of 0.005 mag.

One interesting feature of the Legacy Survey tractor photometry is the provision of ellipticity uncertainties. This catalogue includes ϵ_1 and ϵ_2 for gravitational microlensing analysis where $\epsilon = \sqrt{(\epsilon_1^2 + \epsilon_2^2)}$ and

$$b/a = \frac{1 - \epsilon}{1 + \epsilon}.$$

¹ www.legacysurvey.org

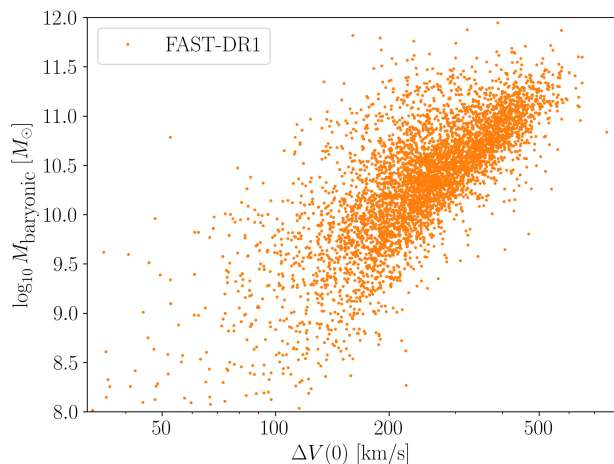


Fig. 1. The baryonic Tully Fisher Relation for the 4,796 FAST galaxies.

From this we obtain by differentiating the the equation for $\cos i$

$$\frac{\delta \sin i}{\sin i} = \frac{(1 - \epsilon)^2}{4 \ln(10)\epsilon(1 + \epsilon)} (\epsilon_1 \delta \epsilon_1 + \epsilon_2 \delta \epsilon_2).$$

For galaxies with $0.2 < b/a < 0.7$, $z < 22$ and half light radius exceeding $3''$ we obtain Figure 1. Clearly all but a few galaxies have $\log \Delta V(0)$ uncertainties from this cause of 0.01 dex, and the modal uncertainty is in the third decimal place.

2.3. DESI-PV data release 1

Said et al. (2024) has released the first sample of peculiar velocities from the DESI survey. The peculiar velocities of galaxies were computed using the Fundamental Plane relation for early-type galaxies and the Tully-Fisher relation for late-type galaxies. During the DESI survey’s validation phase, stellar velocity dispersion data were gathered for 6,698 early-type galaxies. Of these 4,191 were converted to CF4 calibration, none of which were in common with CF4, while a few were in common with FAST; their distances and uncertainties (the latter are similar to the FAST data) were accepted after setting little h to agree with CF4’s (their distances assume $H_0 = 100$).

3. Reconstruction of the CF4++ gravitational velocity field

For simplification in the rest of the article, the catalogue composed of CF4 with the new additions from WALLABY Pilot phase, FAST-DR1, and DESI-PV-DR1 will be referred to as CF4++.

Figure 2 shows the distribution of four datasets in redshift. One can see that FAST-DR1 and WALLABY pilot surveys are mapping the Universe out to velocities of 20,000 km/s, whereas DESI-PV-DR1 extends further out to 30,000 km/s, similar to the SDSS peculiar velocity data previously included in CF4.

In this section we update the local Universe velocity and full matter (dark+luminous) overdensity fields and compare to the previous version using only CF4 datasets (Courtois et al. 2023a).

The animated figure below shows a 3D representation of the variance in the density fluctuation field. Here we show the SGX-SGY plane through SGZ=0 for all our HMC solutions. One can

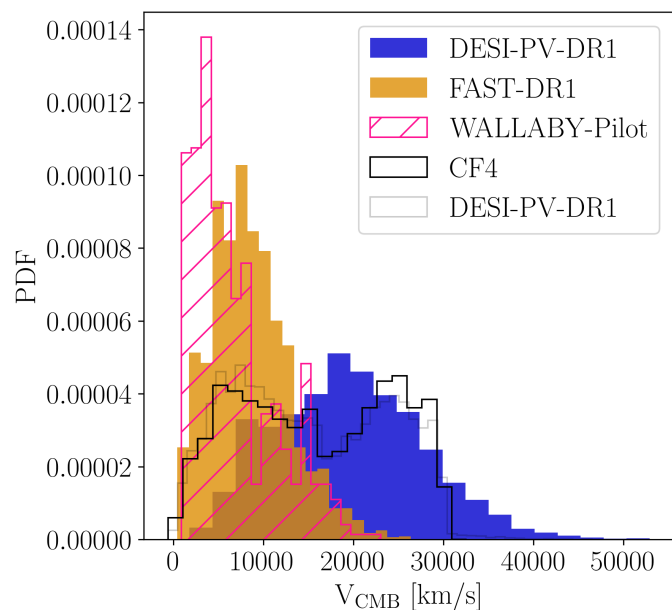


Fig. 2. Distribution in redshift of the four dataset used in this article. FAST-DR1 and WALLABY pilot phase are probing the Universe up to 20,000km/s, while DESI-PV-DR1 extends up to 30,000km/s as did SDSS peculiar velocities that were incorporated in CF4.



Fig. 3. Fluctuations in the Density Field from all HMC realizations of CF4++ through the SGZ=0 plane, can also be viewed here

see that while some of the minor structure appears and disappears, the favoured overdensity regions remain fairly stable as the field evolves.

Figure 4 displays the supergalactic plane in SGX-SGY coordinates. The original Cosmic-Flows catalog data is shown by the black points. The WALLABY Pilot phase, FAST-DR1 and DESI-PV-DR1 galaxies that were integrated into CF4++ are shown as colored circles.

Figure 5 focuses on the nearby Universe in particular on Coma cluster seen at $SGX-SGY=(0;60) h^{-1}\text{Mpc}$ and the Great Attractor region at $SGX-SGY=(-45;0) h^{-1}\text{Mpc}$. The updated cosmography clearly delineates Coma as a stand-alone large scale structure not connected to the Shapley region. The Great Attractor is reinforced as a major contributor to the local density field.

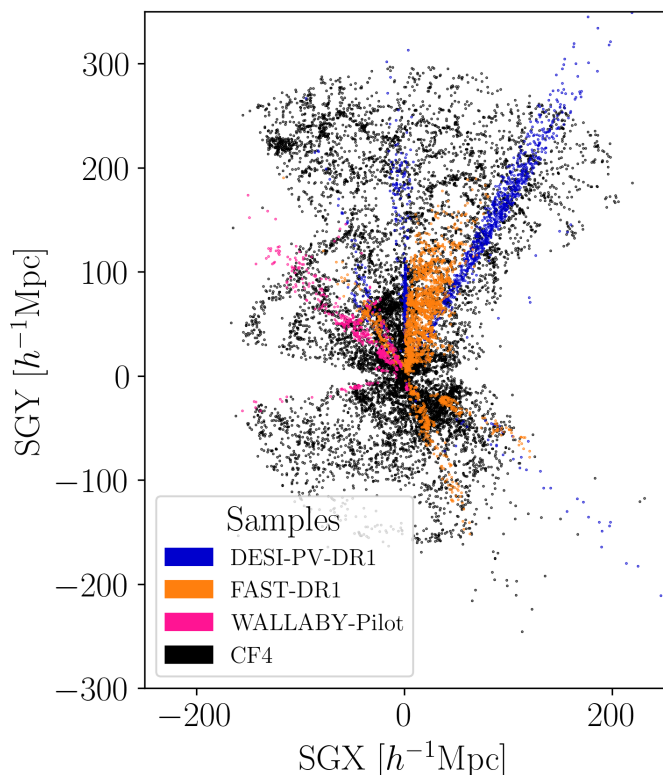


Fig. 4. The distribution of galaxies with measured peculiar velocities in the local Universe, within $z = 0.1$, has been significantly enhanced by the addition of 9,642 galaxy distances. The WALLABY and FAST surveys are extending measurements to approximately $150 h^{-1} \text{Mpc}$, while DESI-PV is expanding coverage to the SDSS limits in the northern terrestrial hemisphere. One can see that the current compilation of galaxy peculiar velocities is highly inhomogeneous, both in sky coverage and data quality. The northern extension of CF4, based on the SDSS-PV sample, is particularly affected by distance-dependent errors, necessitating caution when interpreting flows in that region.

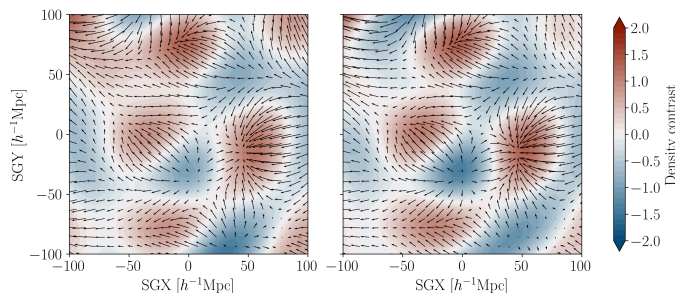


Fig. 5. The CF4 (left) and CF4++ (right) local cosmography. In CF4++ both Coma and the Great attractor now appear as clear stand-alone superclusters, as these structures are clearly split from Shapley which is located at the upper left corner.

Figure 6 focuses on Vela (top) and Shapley (bottom) supercluster regions by presenting the reconstructed matter density contrast based on the CF4 dataset (left) and the CF4++ dataset (right). The CF4 galaxies are marked by black dots, while newly incorporated data points are shown as colored dots. The addition of only very few measurements near the galactic plane reveals the emergence of the Vela supercluster and modifies the density contours of Shapley both in its foreground and background. Shapley is clearly separated from foreground clusters such as Coma or the Great Attractor (Laniakea). Future surveys

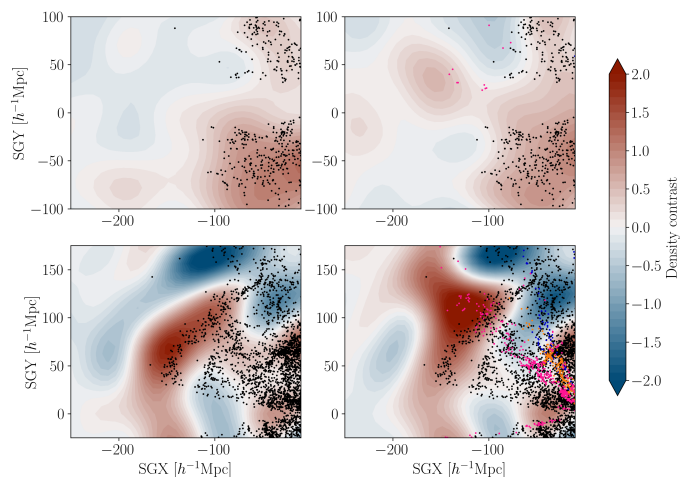


Fig. 6. Focus on Vela (top) and Shapley (bottom) supercluster regions. The figure illustrates the reconstructed matter density contrast derived from the CF4 dataset (left) and the CF4++ dataset (right). Black dots represent the CF4 galaxies, while the colored dots indicate newly added data points. With just a few additional measurements near the galactic plane, the Vela supercluster begins to emerge more clearly. The density contours around Shapley are modified both in its foreground and background. Shapley is clearly separated from the foreground superclusters like Coma and Great Attractor.

and continued observations in this part of the sky will refine our understanding of these massive structures and their significance for near-field cosmology.

4. Bulk flow and homogeneity scale

In order to analyze the Bulk Flow, we first have checked that the dataset was not biased towards a specific environment of the V-web.

The V-web is a method for identifying the cosmic web's structure—voids, walls, filaments, and nodes—using the velocity field of galaxies or matter. It was introduced as an alternative to density-based methods in the context of Local Universe peculiar velocity studies in Tully et al. (2014); Courtois et al. (2015), as well as more recently in the WALLABY survey For et al. (2021); Mould et al. (2024), and in the study of cosmic voids by the CAVITY consortium Courtois et al. (2023c); Conrado et al. (2024). The approach focuses on computing the eigenvalues of the velocity shear tensor, derived from the peculiar velocity field. The tensor captures how velocities change across a region, reflecting the large-scale gravitational dynamics.

By classifying regions based on the eigenvalues, the V-web assigns them to one of the four cosmic web structures. This method emphasizes the dynamical state of the cosmic web rather than static density contrasts, offering a more physically grounded classification. It is particularly advantageous for studying the dynamics of large-scale structure formation and the interplay between matter and gravity over cosmic time.

Figure 7 shows the distribution of the galaxies in the four different V-web settings. Since the Pilot phase of WALLABY focused on galaxy clusters, it does not include galaxies located in cosmic void environments. In contrast, the FAST-DR1 and DESI-PV-DR1 datasets include galaxies spanning all classical cosmic web environments, making them representative of the full range of large-scale structures in the Universe.

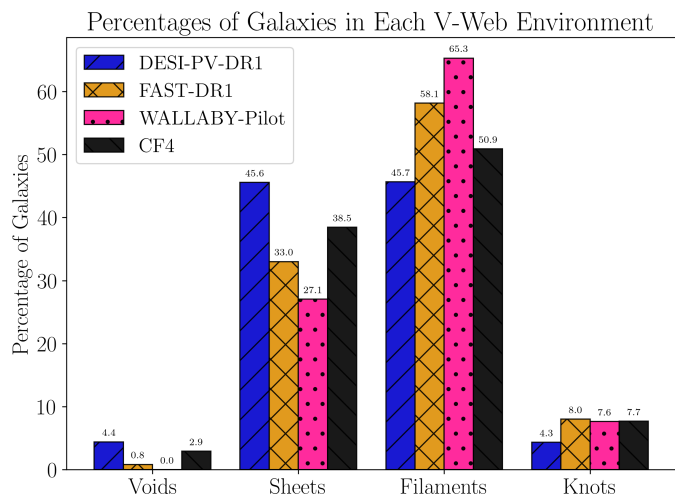


Fig. 7. Distribution of CF4++ galaxies in cosmic-web environments. WALLABY was targeted towards clusters of galaxies. FAST-DR1 and DESI-PV-DR1 are representatives of all cosmic web environments.

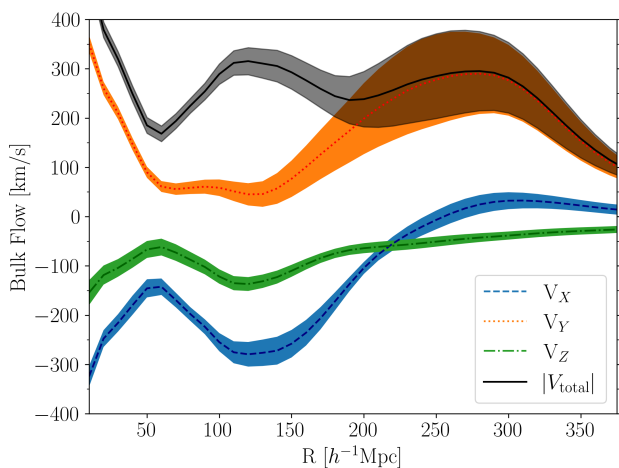


Fig. 8. The mean bulk flow components along the Supergalactic X (blue: dashed), Y (orange: dotted), and Z (green: dash-dotted) axis and the total bulk flow (black: solid), as a function of distance from the observer’s location. The mean and standard deviation (transparent bands) are calculated using the nearly 10 000 HMC realizations.

4.1. Determining the bulk velocity

As peculiar velocity surveys extend to larger scales, it is expected that the overall bulk flow within the observed volume will tend toward zero when compared to the reference frame established by the CMB. The extent to which this bulk flow diminishes in relation to survey volume serves as an indicator of large-scale modes of the matter power spectrum and density field. Given that the velocity fields are evaluated on a 3D Cartesian grid, the bulk velocity components can be easily determined as the volume-weighted average velocity within a top-hat sphere of radius R as follows:

$$\mathbf{V}_{\text{bulk}}(R) = \frac{3}{4\pi R^3} \int_{x < R} \mathbf{v}(\mathbf{x}) d^3x \quad (1)$$

Figure 8 presents the amplitude of the total bulk flow (black) as a function of distance from the observer’s position, along with the three Cartesian components (coloured) along the Supergalac-

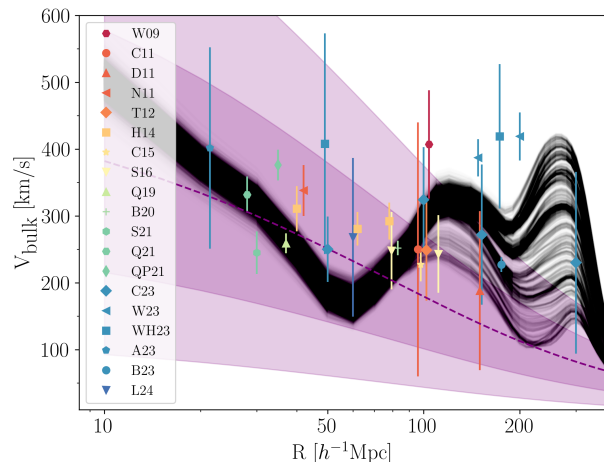


Fig. 9. The total bulk flow of each HMC CF4++ realization (black), as a function of distance. Overplotted are the Table 1 values assuming an effective radius corresponding to a spherical top-hat window function, and the dashed curved line is the corresponding linear theory Λ CDM prediction. The light and dark regions represent the 1σ and 2σ confidence levels, respectively. Small offsets have been introduced in the cases of overlapping data points.

tic X, Y, and Z axes. Shown here are the mean and standard deviation of our HMC realizations, as expected at larger distances, with increasing homogeneity of the Universe, the bulk flow tends towards zero. Our 3D HMC realizations are significantly affected by abrupt declines in the number of galaxies observed, as these reductions can lead to incomplete or biased sampling of the cosmic structure. We find that radii associated with sharp decreases in galaxy counts correspond to the radii with increased variability in the velocity fields and hence our recovered bulk flows. This is especially true for the SGY-component of the bulk flow as the data is heavily skewed in favour of the +SGY component, whereas the both the SGX and SGZ components are significantly more symmetrical in distribution. This imbalance in the current dataset is hence reflected in our measurements of the bulk flow and the amount of standard deviation therein.

4.2. Comparison of recent measurements with Λ CDM predictions

As the amplitude of the bulk flow, $|\mathbf{B}|$, is sensitive to the matter power spectrum’s large-scale modes, for a given cosmological model the measured bulk flow can thus be compared with the predicted value. The expected mean of the bulk flow is zero, as statistically the Universe is homogeneous and isotropic. However, the root-mean-square variance of the bulk flow amplitude, provides insight into our local Universe as it is dependent on the matter power spectrum $P(k)$, the scale R , as well as the window function $W(R)$ in which it is measured.

Over the past 15 years, various studies have investigated the bulk flow. We present a summary of these values and their quoted distances in Table 1. While some studies report values exceeding those predicted by Λ CDM (notably, Watkins et al. 2023; Whitford et al. 2023, recently), others find no significant differences from expectations. Which assuming linear perturbation theory, the variance of the bulk flow at a given scale, is given by:

$$\sigma_{\text{BF}}^2(R) = \langle \mathbf{B}^2 \rangle = \frac{H_0^2 f^2}{2\pi^2} \int_0^\infty P(k) \tilde{W}^2(k; R) dk \quad (2)$$

where $\tilde{W}(k)$ is the Fourier transform of the window function (Gorski 1988). In this work, we use the publicly available python CAMB package to calculate the linear matter power spectrum (Lewis et al. 2000), and assume a spherical top-hat window function, such that $\tilde{W}(k; R) = 3(\sin(kR) - kR \cos(kR))/(kR)^3$.

Assuming the density field is Gaussian, the peculiar velocity field is then given by the Maxwellian distribution and the png can be estimated using (Bahcall et al. 1994):

$$p(|\mathbf{B}|) = \sqrt{\frac{2}{\pi}} \left(\frac{3}{\sigma_{\text{BF}}^2} \right)^{3/2} |\mathbf{B}|^2 \exp\left(-\frac{3|\mathbf{B}|}{2\sigma_{\text{BF}}^2}\right), \quad (3)$$

where the most probable \mathbf{B} is $B = \sqrt{2/3}\sigma_{\text{BF}}$, and the 1 and 2σ confidence levels of the cosmic variance of \mathbf{B} are $B_{-0.619\sigma_{\text{BF}}}^{+0.419\sigma_{\text{BF}}}$ and $B_{-0.619\sigma_{\text{BF}}}^{+0.891\sigma_{\text{BF}}}$ (Scrimgeour et al. 2016).

To accurately compare measurements from specific datasets with the theoretical predictions of Λ CDM, requires one to account for any potentially complex survey window function. However, to facilitate comparisons across different datasets, it is essential to standardize this window function. In Figure 9, we compare our bulk flow amplitude of each CF4++ HMC realization as a function of distance from the observer, against previous measurements, and the Λ CDM prediction assuming a spherical top-hat window. The values quoted in Table 1 that were calculated using an alternative window function, are adjusted to a new effective radius (R_e), following the methodology in Scrimgeour et al. (2016). Measurements which were calculated based on a Gaussian filter, are plotted at $R_e = 2R$ to align them more closely with the predictions of the spherical top-hat window. Similarly, the values presented in Scrimgeour et al. (2016) use a Gaussian filter and are based on the 6dFGSv survey which is akin to a hemispherical top-hat, so following their arguments we plot their quoted values at $R_e = 2(R^3/2)^{1/3}$. If the methodology used to calculate the effective radius of the bulk flow measurement was unstated in the original paper we make no corrections and measurements are placed at their reported bulk flow depths.

In regards to these previous studies, we find no significant trend for the recovered bulk flow, neither in terms of recency of the study nor the data used in each measurement. Within a distance of $150 h_{100}^{-1}$ Mpc, Courtois et al. (2023a) measurements indicates that CF4 exhibits a bulk flow of $230 \pm 136 \text{ km s}^{-1}$. While our measurements of the bulk flow at $R > 100$ slightly higher than what is predicted by Λ CDM they are still consistent with current predictions and with previous measurements of the bulk flow.

5. Conclusions

This study provides an updated cosmography of the local Universe within $z = 0.1$, incorporating new galaxy peculiar velocity datasets from preliminary data-releases of WALLABY, FAST, and DESI surveys. This enhanced dataset, referred to as CF4++, includes 9,642 additional galaxy distances, allowing for a more detailed analysis of the local Universe's bulk flow dynamics and structure.

Key conclusions from the study include:

- the bulk flow, which represents the coherent motion of galaxies due to gravitational interactions, was analyzed using the CF4++ dataset. The study found that the bulk flow amplitude tends to zero at larger distances, indicating increasing homogeneity of the Universe. Within a distance of $150 h^{-1}$ Mpc, the bulk flow measured is $230 \pm 136 \text{ km s}^{-1}$, consistent with previous measurements and predictions from the Λ CDM cosmological model.

The study observed that the bulk flow measurements are slightly higher than predicted by Λ CDM but still within the expected range, suggesting no significant deviations from the standard cosmological model;

- the updated cosmography reveals more spherical shapes and clearly defined boundaries for key regions such as the Great Attractor (Laniakea) and Coma superclusters. The study highlights the emergence of the Vela supercluster with the addition of new measurements, emphasizing the importance of continued observations in this region.

Overall, the integration of new datasets into the CF4++ catalog shows that the dynamical scale of homogeneity is not yet reached within the interval $[200-300] h^{-1}$ Mpc from the observer, indicating that the local Universe still exhibits significant fluctuations in the distribution of mass and dynamics of galaxy motions. Future surveys and continued observations will further refine this cosmography and contribute to a more comprehensive understanding of the Universe's structure and evolution.

Data Availability

These data are all publicly available. More data tables are at <https://github.com/jrmould/fast>.

Acknowledgements. AD is supported by a KIAS Individual Grant PG 087201 at the Korea Institute for Advanced Studies. HMC acknowledges support from the Institut Universitaire de France and from Centre National d'Etudes Spatiales (CNES), France. JRM received support from the ARC CoE Centre for Dark Matter Particle Physics (CDM, CE200100008). This research used services and data provided by the Astro Data Lab at NSF's National Optical-Infrared Astronomy Research Laboratory. Details are given in the github URL above.

References

- Avila, F., Oliveira, J., Dias, M. L. S., & Bernui, A. 2023, *Brazilian Journal of Physics*, 53, 49
- Bahcall, N. A., Gramann, M., & Cen, R. 1994, *The Astrophysical Journal*, 436, 23
- Boruah, S. S., Hudson, M. J., & Lavaux, G. 2020, *MNRAS*, 498, 2703
- Boubel, P., Colless, M., Said, K., & Staveley-Smith, L. 2024, *MNRAS*, 531, 84
- Carrick, J., Turnbull, S. J., Lavaux, G., & Hudson, M. J. 2015, *MNRAS*, 450, 317
- Colin, J., Mohayaee, R., Sarkar, S., & Shafieloo, A. 2011, *MNRAS*, 414, 264
- Conrado, A. M., González Delgado, R. M., García-Benito, R., et al. 2024, *A&A*, 687, A98
- Courtois, H. M., Dupuy, A., Guinet, D., et al. 2023a, *A&A*, 670, L15
- Courtois, H. M., Said, K., Mould, J., et al. 2023b, *MNRAS*, 519, 4589
- Courtois, H. M., van de Weygaert, R., Aubert, M., et al. 2023c, *A&A*, 673, A38
- Courtois, H. M., Zaritsky, D., Sorce, J. G., & Pomarède, D. 2015, *MNRAS*, 448, 1767
- Dai, D.-C., Kinney, W. H., & Stojkovic, D. 2011, *J. Cosmology Astropart. Phys.*, 2011, 015
- Drlica-Wagner, A., Ferguson, P. S., Adamów, M., et al. 2022, *ApJS*, 261, 38
- For, B. Q., Wang, J., Westmeier, T., et al. 2021, *MNRAS*, 507, 2300
- Gorski, K. 1988, *ApJ*, 332, L7
- Haynes, M. P., Giovanelli, R., Kent, B. R., et al. 2018, *ApJ*, 861, 49
- Hoffman, Y., Courtois, H. M., & Tully, R. B. 2015, *MNRAS*, 449, 4494
- Hong, T., Springob, C. M., Staveley-Smith, L., et al. 2014, *MNRAS*, 445, 402
- Koribalski, B. S., Staveley-Smith, L., Westmeier, T., et al. 2020, *Ap&SS*, 365, 118
- Lewis, A., Challinor, A., & Lasenby, A. 2000, *ApJ*, 538, 473
- Lima-Dias, C., Monachesi, A., Torres-Flores, S., et al. 2021, *MNRAS*, 500, 1323
- Lopes, M., Bernui, A., Franco, C., & Avila, F. 2024, *ApJ*, 967, 47
- Ma, Y.-Z. & Scott, D. 2013, *MNRAS*, 428, 2017
- Mould, J., Jarrett, T. H., Courtois, H., et al. 2024, *MNRAS*, 533, 925
- Moustakas, J., Lang, D., Dey, A., et al. 2023, *ApJS*, 269, 3
- Murugesan, C., Deg, N., Westmeier, T., et al. 2024, *PASA*, 41, e088
- Nusser, A. & Davis, M. 2011, *ApJ*, 736, 93
- Qin, F. 2021, *Research in Astronomy and Astrophysics*, 21, 242
- Qin, F., Howlett, C., Staveley-Smith, L., & Hong, T. 2019, *MNRAS*, 482, 1920
- Qin, F., Parkinson, D., Howlett, C., & Said, K. 2021, *ApJ*, 922, 59
- Said, K., Howlett, C., Davis, T., et al. 2024, *arXiv e-prints*, arXiv:2408.13842

Distance : Selection Function	Dataset(s)	0-50 h^{-1} Mpc	51-100 h^{-1} Mpc	100-150 h^{-1} Mpc	>150 h^{-1} Mpc
predicted Λ CDM		300 km/s	200 km/s	190 km/s	100 km/s
expected Cosmic Variance		300 km/s	200 km/s	100 km/s	60 km/s
W09 : Gaussian	SFI++, SN, etc.	407 \pm 81 (50)			
C11 : Top-Hat	Union 2 SN		250 \pm 190 (100)		
D11 : Top-Hat	Union 2 SN			188 \pm 119 (150)	
N11 : Top-Hat	SFI++	333 \pm 38 (40)			
T12 : Gaussian	A1SN	249 \pm 76 (50)			
M13 : Top-Hat	SFI++, A1SN, etc.	310 (50)			
H14 : Gaussian	2MTF	292 \pm 28 (40)			
C15 : Gaussian	2M++	227 \pm 25 (50)			
H15 : Top-Hat	CF2	250 \pm 21 (50)		239 \pm 38 (150)	
S16 : Hemisphere	6dFGSv	248 \pm 58 (50)	243 \pm 58 (70)		
Q19 : Top-Hat	2MTF, CF3	259 \pm 15 (37)			
B20 : Gaussian	A2SN, SFI++	252 \pm 11 (40)			
S21 : Top-Hat	DSS	245 \pm 32 (30)			
Q21 : Top-Hat	2MTF	332 \pm 27 (30)			
QP21 : Top-Hat	CF4TF	376 \pm 23 (35)			
C23 : Top-Hat	CF4	250 \pm 49 (50)	324 \pm 79 (100)	272 \pm 105 (150)	230 \pm 136 (300)
A23 : Top-Hat	ALFAFA	401 \pm 151 (21)			
W23 : -	CF4			395 \pm 29 (150)	427 \pm 37 (200)
WH23 : Top-Hat	CF4	408 \pm 165 (49)			428 \pm 108 (173)
B24 : -	CF4				227 \pm 11 (175)
L24 : -	SN-Pantheon+		268 \pm 119 (61)		
This Work: Top-Hat	CF4++	185 \pm 16 (50)	289 \pm 21 (100)	292 \pm 34 (150)	238 \pm 56 (200)

Table 1. Bulk Flow measurements in the literature using supernovae or galaxy peculiar velocity datasets (W09: Watkins et al. (2009), C11: Colin et al. (2011), D11: Dai et al. (2011), N11: Nusser & Davis (2011), T12: Turnbull et al. (2012), M13: Ma & Scott (2013), H14: Hong et al. (2014), C15: Carrick et al. (2015), H15: Hoffman et al. (2015), S16: Scrimgeour et al. (2016), Q19: Qin et al. (2019), B20: Boruah et al. (2020), S21: Stahl et al. (2021), Q21: Qin (2021), QP21: Qin et al. (2021), C23: Courtois et al. (2023a), A23: Avila et al. (2023), W23: Watkins et al. (2023), WH23: Whitford et al. (2023), B24: Boubel et al. (2024), L24: Lopes et al. (2024)). The radii listed in brackets this table are the stated values of their respective texts in units of h^{-1} Mpc, those with selection functions which are *non* Top-Hat are modified using the methodology described in Section 4 when plotted in Figure 9. The Λ CDM and cosmic variance values quoted at the top of the table are the measurements expected at 50, 100, 150 and 300 h^{-1} Mpc., respectively

Schlafly, E. F. & Finkbeiner, D. P. 2011, ApJ, 737, 103
 Scrimgeour, M. I., Davis, T. M., Blake, C., et al. 2016, MNRAS, 455, 386
 Stahl, B. E., de Jaeger, T., Boruah, S. S., et al. 2021, MNRAS, 505, 2349
 Taylor, E. N., Hopkins, A. M., Baldry, I. K., et al. 2015, MNRAS, 446, 2144
 Tully, R. B., Courtois, H., Hoffman, Y., & Pomarède, D. 2014, Nature, 513, 71
 Turnbull, S. J., Hudson, M. J., Feldman, H. A., et al. 2012, MNRAS, 420, 447
 Watkins, R., Allen, T., Bradford, C. J., et al. 2023, MNRAS, 524, 1885
 Watkins, R., Feldman, H. A., & Hudson, M. J. 2009, MNRAS, 392, 743
 Westmeier, T., Deg, N., Spekkens, K., et al. 2022, PASA, 39, e058
 Whitford, A. M., Howlett, C., & Davis, T. M. 2023, MNRAS, 526, 3051
 Zhang, C.-P., Zhu, M., Jiang, P., et al. 2024, Science China Physics, Mechanics, and Astronomy, 67, 219511